

A Parallel Algorithm for Studying the Ice Cover Impact onto Seismic Waves Propagation in the Shallow Arctic Waters

Galina Reshetova ✉^{1,2}, Vladimir Cheverda², Vadim Lisitsa², and Valery Khaidykov²

¹ Institute of Computational Mathematics and Mathematical Geophysics SB RAS, Novosibirsk 630090, Russia

✉ kgv@nmsf.ssc.ru

² Trofimuk Institute of Petroleum Geology and Geophysics SB RAS, Novosibirsk, Russia

{ CheverdaVA, LisitsaVV, KhaidykovVG }@ipgg.sbras.ru

Abstract. The seismic study in the Arctic transition zones in the summer season is troublesome because of the presence of large areas covered by shallow waters like bays, lakes, rivers, their estuaries and so on. The winter season is more convenient and essentially facilitates logistic operations and implementation of seismic acquisition. However in the winter there is another complicating factor: intensive seismic noise generated by sources installed on the floating ice. To understand peculiarities of seismic waves and the origin of such an intensive noise, a representative series of numerical experiments has been performed. In order to simulate the interaction of seismic waves with irregular perturbations of underside of the ice cover, a finite-difference technique based on locally refined in time and in space grids is used. The need to use such grids is primarily due to the different scales of heterogeneities in a reference medium and the ice cover should be taken into account. We use the domain decomposition method to separate the elastic/viscoelastic model into subdomains with different scales. Computations for each subdomain are carried out in parallel. The data exchange between the two groups of CPU is done simultaneously by coupling a coarse and a fine grids. The results of the numerical experiments prove that the main impact to noise is multiple conversions of flexural waves to the body ones and vice versa and open the ways to reduce this noise.

Keywords: Seismic waves · Transition zones · Finite-difference schemes · Local grid refinement · Domain decomposition.

1 Introduction and Motivation

One of the distinctive features of the Russian Far North (Fig. 1a) is the presence of large areas covered by shallow waters which bring a lot of troubles when implementing of seismic observations in the summer (Fig. 1b). At the same time,

2 G. Reshetova et al.

in the winter these shoals are overlapped by the thick ice (up to a few meters), which significantly facilitates logistic operations and can be used to install seismic sources (Fig. 1c). It is worth mentioning that potential advantages of conducting seismic operations on the winter ice are motivating numerous investigations of the feasibility of shooting seismic from the ice cover [1]. In Fig. 2, one can see two field seismograms: for the onshore source position (Fig. 2a) and for a source placed onto the ice (Fig. 2b). Comparison of these seismograms reveals a high noise in seismic data for ice-placed sources, whereas their quality for land-based groups is quite acceptable and one can see the target reflections there even without preprocessing. Let us also pay attention to a sharp disappearance of the noise in Fig. 2b at a distance of 1000 m to the left from the source. In this place, the ice cover meets a solid ground (permafrost). It is well known that this

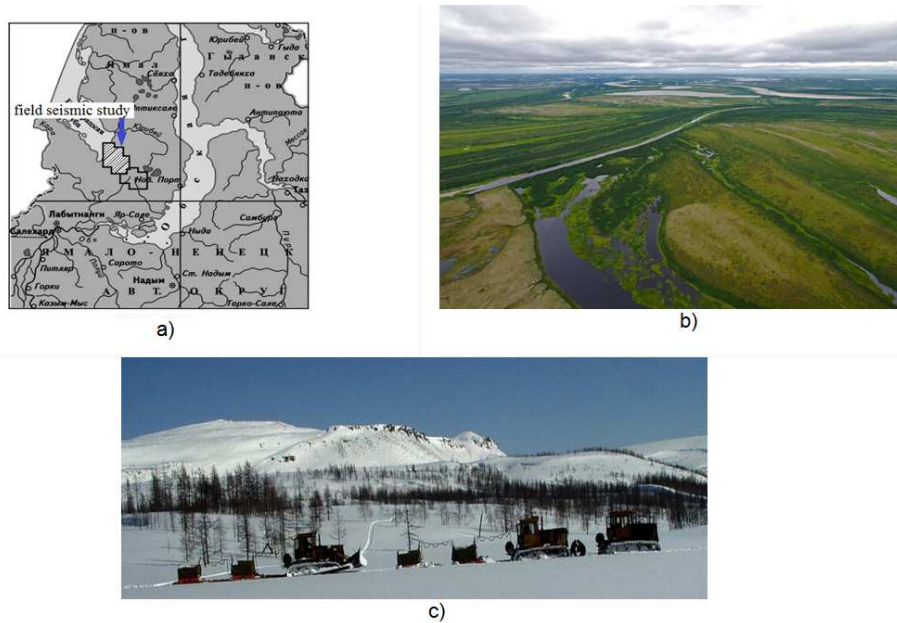


Fig. 1. a) Geography of seismic field observations. b) Top view of the area in summer. c) The same area in winter.

noise is associated with flexural waves generated in the ice by seismic sources. These waves are one of the strongest known coherent noises. At the same time, such waves are much slower than the surface waves and seem to be easy canceled by f-k filtration. However, this type of filtration fails to suppress such a noise.

There are some intuitive explanations of this fact, in particular, the bending of the ice produced by the impulse seismic source which generates multiples in the shallow water column as well as weakening of a signal by transferring the ice-water-mud interfaces. To understand the peculiarities of seismic waves and

the origin of this high noise, a representative series of numerical experiments have been performed by means of a careful finite-difference simulation.

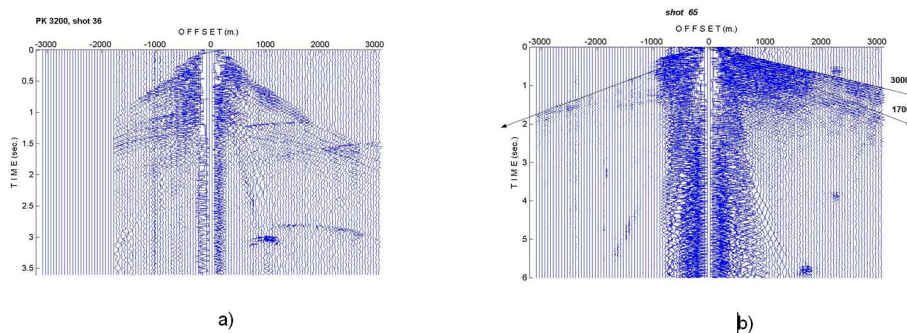


Fig. 2. Field seismograms. a) Onshore source position. b) Source on an iced shoals.

2 Mathematical Formulation

Our main suggestion is that the noise in seismograms is caused mainly by the flexural waves [5], [8], and we are going to use the numerical simulation to justify this point. To do this, we use the Generalized Standard Linear Solid (GSLs) model [2] governing the seismic wave propagation in viscoelastic media: where ρ is the mass density; C_1 and C_2 are fourth order tensors, defining the model properties; u is the velocity vector; σ and ε are the stress and strain tensors, respectively; r^l are the memory variables. Note that the number of memory variable is L , which is typically two or three. The proper initial and boundary conditions are assumed.

3 Numerical Method

An explicit finite-difference standard staggered grid scheme (SSGS) approximating elastic/viscoelastic wave equations in the velocity-stress formulation with parameters modification is used to solve the problem. This numerical technique combines a high efficiency with a suitable accuracy [9], [10].

We consider GSLs equations in order to take into account the seismic attenuation in the ice filling of the uppermost part of the model. For the ideal-elastic lower part of the model, the tensor C_2 is zero. Thus, memory variables do not appear in the equations in this area, and the system turns into that for an ideal-elastic wave equation.

4 G. Reshetova et al.

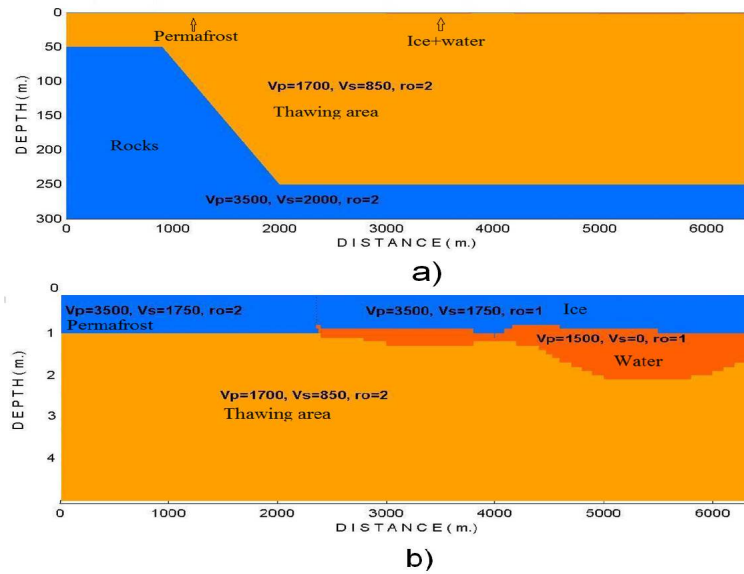


Fig. 3. The vertical slice of 3D realistic model of a shoal covered by the ice. a) Middle scale depth b) Shallow part.

4 Fitting a Geological Model to Data

To fit a geological model to real seismic data we have started with a simple 3D three layer ice/water/ground model, which possesses all the key components of the real life: solid ground with and without permafrost, ice, water and thawing area under water. The model was prepared together with experienced geologists and is presented in Fig. 3a (middle scale in depth) and Fig. 3b (the uppermost part of the model). A synthesized vertical component is presented in Fig. 4. As one can see, all waves are properly positioned and have a predicted behavior. However, the structure of the vertical component of the synthetic data considerably differs from the field observations.

The next modification of the model had the irregular underside of the ice imbedded into the previous model. The idea was found from the research of the U.S. Geological Survey. In the 1960-s they conducted a series of the winter research into the underside of the ice in the basin of the low St. Croix River, Wisconsin (see Fig. 5 presented in [3]). The measurements prove that typical scales of the water-ice interface are about 0.5 m x 0.5 m x 0.05m. Hydrologically this area is similar to the Yamal peninsula and possesses approximately the same structure of the currents (compare with Fig. 2), but the latter is much farther to the north, hence, the winter season is much cooler and the ice is thicker. Therefore in the numerical experiments, perturbations of the underside of the ice was doubled and taken as a random distribution of 2 m x 2 m x 0.1m prisms, which can be seen in Fig. 6. The vertical component of the synthetic seismogram

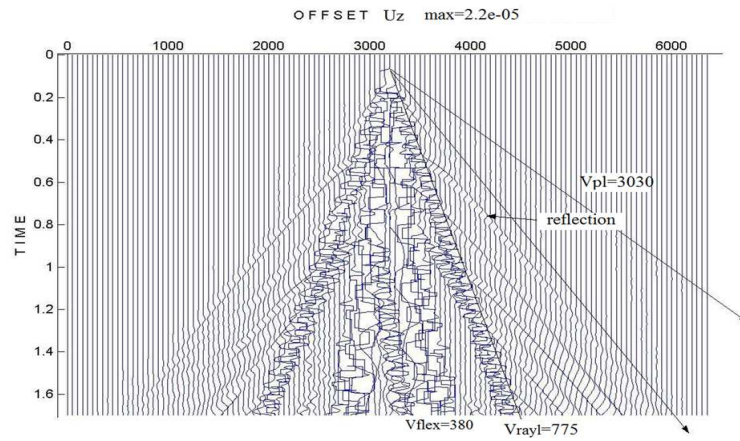


Fig. 4. The vertical displacement component of the on the free surface. One can clearly see all types of elastic waves.

for this model is presented in Fig. 7. Let us note that now it fits rather well to the real life field data, that is, there is a strong dispersive component which overlaps the target reflections. At the same time, for the receivers placed on the solid ground this noise disappears. Base on this fact the following conclusion can be made: the noise for seismic acquisitions onto the ice is associated with random perturbations of the ice/water interface.

5 Optimization of Computations

Let us indicate the upper part of the model as a subdomain Ω_1 (Fig. 6), where the full viscoelastic wave equation is used, while the remaining part of the medium Ω_2 is ideal-elastic.

The upper part of the geological model contains small-scale heterogeneities described by random perturbations of the ice-water interface and leads to representation with an extremely excessive detail. The straightforward implementation of finite-difference techniques brings about the necessity of using dramatically small grid steps to match the scale. From the computational point of view, this means a huge amount of memory required for the simulation and, therefore, extremely large computation time, even with the use of modern high-performance computers.

Our solution to this issue is to use two levels of optimization:

- To use the coupling of different elastic/viscoelastic equations, that is, different governing elastic/viscoelastic equations in subdomains Ω_1 and Ω_2 . The local use of computationally expensive viscoelastic equations only in a narrow part of the subdomain Ω_1 of the model can essentially speed-up the simulation ;

6 G. Reshetova et al.

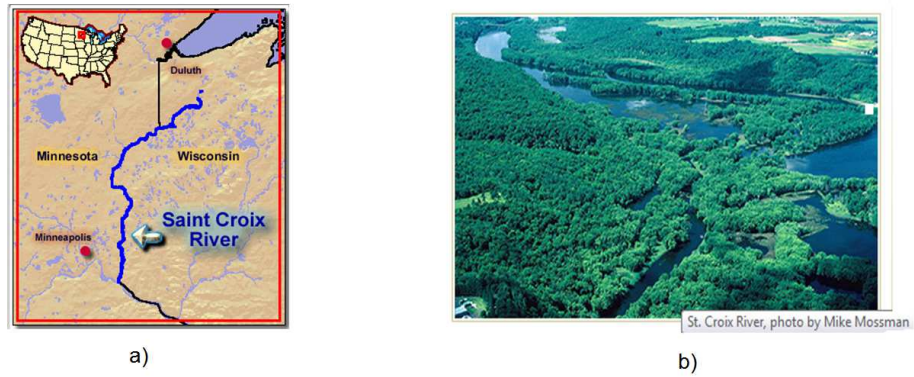


Fig. 5. The St. Croix river. a) Map b) Photo.

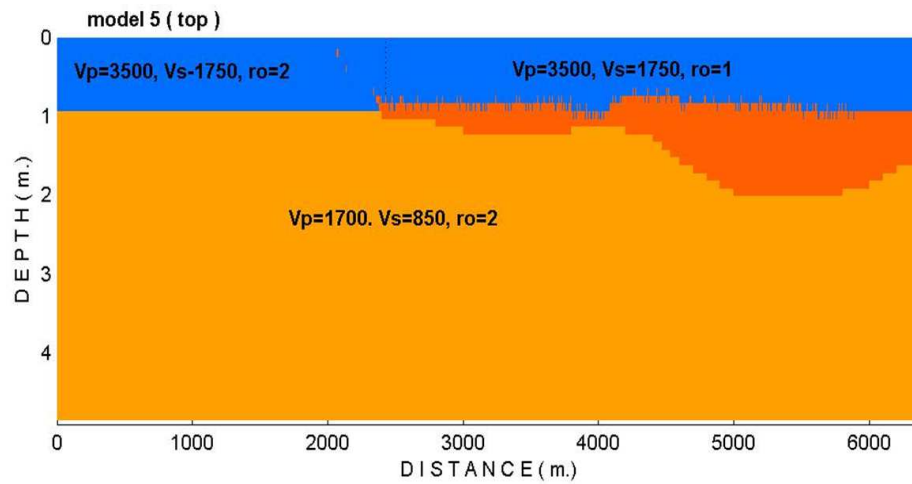


Fig. 6. The uppermost part of the 3D model slice with random perturbations of the ice-water interface (compare with Fig. 3).

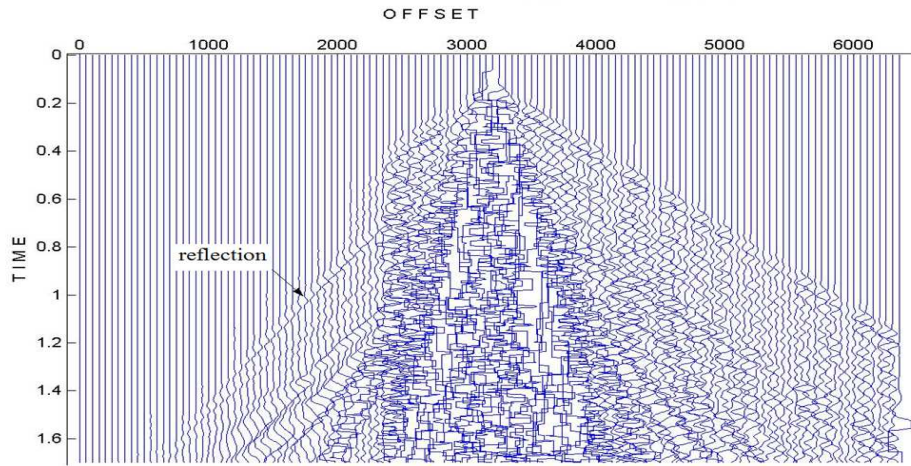


Fig. 7. Synthetic seismograms for the model presented in Fig. 6. Note strong partially correlated dispersive noise beneath the ice.

- To use multi-scale simulation, that is, different mesh sizes to describe different parts of the model: a coarse grid for the background model Ω_2 and a fine grid for describing the area Ω_1 .

Let us take a closer look at each of the levels.

5.1 Coupling of Different Elastic/Viscoelastic Equations

Assume a subdomain Ω_1 , where the full viscoelastic wave equation is used, while the ideal-elastic wave equation is valid over the rest of the space Ω_2 . It is easy to prove that the conditions at the interface $\Gamma = \partial \Omega_1$ are the following:

$$[\sigma \cdot \mathbf{n}]|_{\Gamma=0}, \quad [u]|_{\Gamma=0}, \quad (1)$$

where \mathbf{n} is the outward normal vector and $[f]$ denotes a jump of the function f at the interface Γ . These conditions are the same as those for the elastic wave equation at the interface. In our case, when the SSGS scheme is used, these conditions are automatically satisfied [7]. Thus, the coupling of different elastic/viscoelastic equations does not require any special treatment of conditions at the interface and can be implemented by allocating RAM for memory variables and solving equations for them only in the viscoelastic part of the model.

5.2 Multi-Scale Simulation

A local mesh refinement is used only in the domain Ω_1 with a fine structure to perform the full waveform simulation of the long wave propagation through a model [6]. As was mentioned above, when an explicit finite differences are used,

the size of a time step strongly depends on the spatial discretization, and so the time stepping should be local. As a result, the problem of the simulation of seismic wave propagation in models containing small-scale structures becomes a mathematical problem of a local time-space mesh refinement.

Let us consider how a coarse and a fine grids are coupled. The necessary features of the finite difference method, based on a local grid refinement, are the stability and an acceptable level of artificial reflections. The scattered waves have an amplitude of about 1% of the incident wave, thus the artifacts should be at most 0.1% of the incident wave. If we refine the grid simultaneously in time and in space, then the stability of the finite difference schemes can be provided via the coupling of a coarse and a fine grids based on the energy conservation, which bring about an unacceptable level (exceeding 1%) of artificial reflections [4]. We modify this approach so that the grid is refined in time and in space in turn on two different surfaces surrounding the target area Ω_1 with a microstructure.

Refinement in Time We present refinement with respect to time with a fixed 1D spatial discretization in Fig.8. Its modification for 2D and 3D is straightforward.

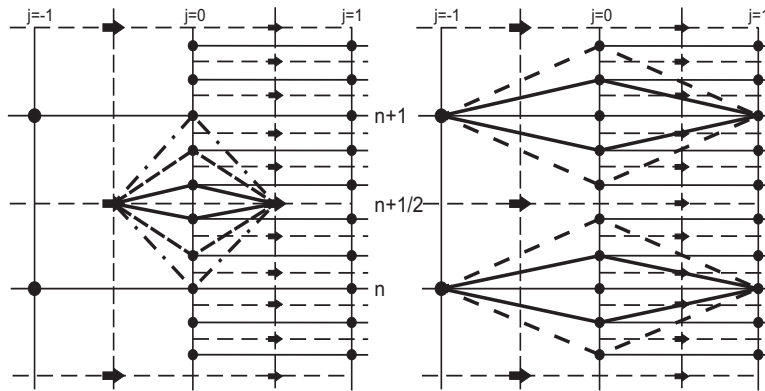


Fig. 8. Embedded stencils for the local time stem mesh.

Refinement in Space In order to change the spatial grids, a FFT-based interpolation is used. Let us schematically explain the procedure. The mutual disposition of a coarse and a fine spatial grids one can see in Fig.9, which corresponds to updating the stresses. As can be seen, to update the solution on a fine grid on the uppermost line it is necessary to know the wavefield at the points marked in black, these points not existing on a given coarse grid. Using the fact that all of the points are on the same line (plane in 3D), we seek for the values of missing nodes by the FFT-based interpolation. This procedure allows us to

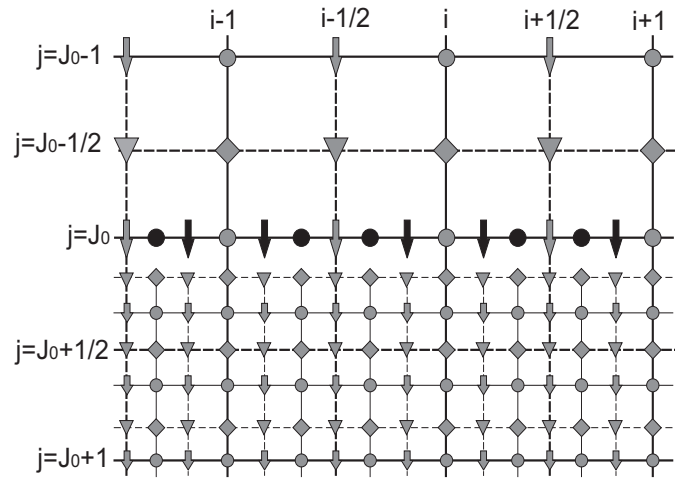


Fig. 9. Spatial steps refinement. Black marks correspond to points where the coarse-grid solution is interpolated.

provide a required low level of artifacts (about 0.001 with respect to the incident wave) generated at the interface of these two grids.

6 Parallel Computations

The parallel implementation of the algorithm has been carried out using the static domain decomposition.

The use of the local space-time grid stepping makes it difficult to ensure a uniform work load for Processor Units (PU) in the domain decomposition.

The parallel computation is implemented using two groups of processors. The 3D heterogeneous background (a coarse grid Ω_2) is placed into one group, while the fine mesh describing Ω_1 is distributed in the other group. There is a need for interactions between processors within each group and between the groups as well. The data exchange within a group is done via faces of the adjacent subdomains by non-blocking iSend/iReceive MPI procedures. The interaction between the groups is designed for coupling a coarse and a fine grid.

From Coarse to Fine The processors aligned to the coarse grid are grouped along each of the face in contact with the fine grid. At each of the faces a Master Processor (MP) gathers the computed current values of stresses/displacements, applies FFT and sends a part of the spectrum to the relevant MP on a fine grid (see fig.10). All the subsequent data processing, i.e. interpolation and inverse FFT, is performed by the relevant MP in the fine grid group. Subsequently, this MP sends the interpolated data to each processor in its subgroup.

Exchange of a part of FFT spectrum and interpolation performed by the MP of the second group essentially decreases the amount of sent/received data and, hence, idle time.

From Fine to Coarse Processors from the second group compute the solution on the fine grid. For each face of the fine grid block, a MP is identified. This MP collects data from the relevant face, performs FFT, and sends a part of the spectrum to the corresponding MP of the first group (a coarse grid). Formally, FFT can be excluded and the data to be exchanged can be obtained as a projection of the fine grid solution onto the coarse grid, however the use of truncated spectra reduces the amount of data to be exchanged and ensures stability as it acts as a high-frequency filter. Finally, the interpolated data are sent to the processors

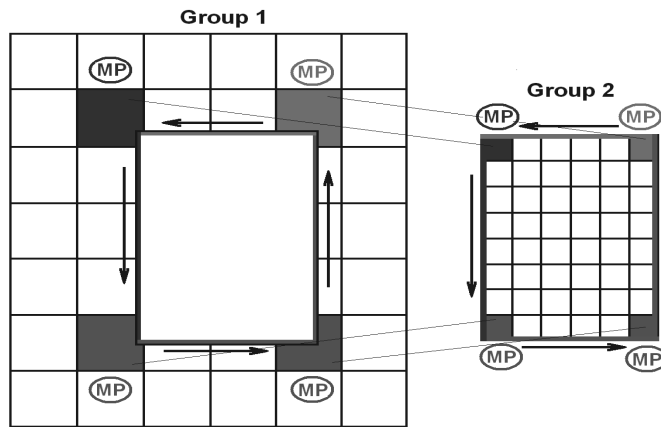


Fig. 10. Processor Units for a coarse (left) and a fine (right) grids.

which need these data. The use of non-blocking procedures `Isend/Irecv` allow performing communications during updating the solution in the interior of the subdomains, thus a weak scaling of the algorithm is close to 93% for the use of up to 4000 cores.

7 Possible Solutions to Reduce the Noise

One of the possible solutions to reduce the noise-to-signal ratio can be to slit the ice separating sources and receivers [5]. This slit stops asymmetric modes of the flexural waves and kills noise in the data beyond the slit. This effect is clearly seen in Fig. 11b as a remarkable damping of flexural waves. Another way to weaken flexural waves may be the construction of rib stiffness, some kind of artificial ice hummock. This will stiffen the ice and weaken flexural modes. The geometry of this rib can be chosen by numerical experiments. In contrast to the slit, such a hummock is cheaper and can be erected very quickly.

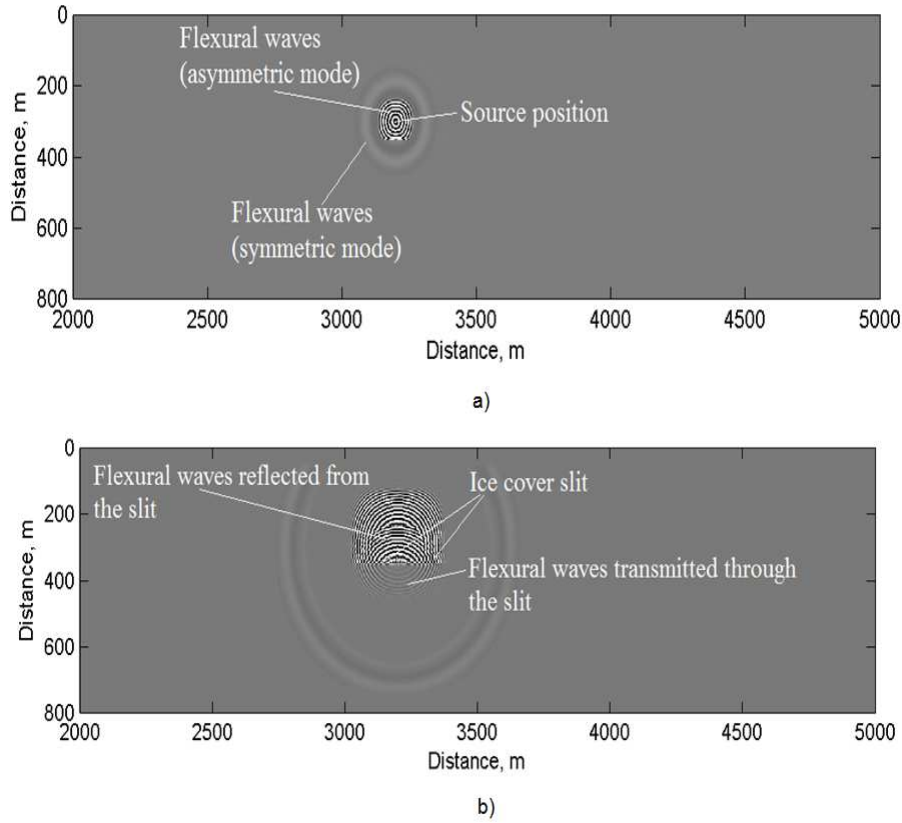


Fig. 11. Top view of the vertical component in the presence of a slit through the ice.

8 Conclusion

We have presented an original algorithm for the numerical simulation of seismic waves propagation in complex 3D media. The main idea of the approach proposed is the hybrid elastic/viscoelastic algorithm based on the local time-space mesh refinement. The use of independent domain decomposition for different regions with different system of equations and grid refinements results in a well-balanced algorithm and reduces need for of the computational resources up to several orders if compared with the fine grid simulations.

This approach was applied to simulate the interaction of seismic waves with irregular perturbations of the underside of the ice cover in order to understand the main peculiarities of seismic waves and the origin of a high seismic noise generated for acquisitions installed on the ice covering shallow waters.

A representative series of numerical experiments for realistic 3D models with allowance for the shape of the ice cover, bathymetry, permafrost and thawing area

12 G. Reshetova et al.

have revealed the following roots of this noise:

- the vertical force generates intensive flexural waves which interact with heterogeneities of the ice-water interface and convert to fast symmetric modes;
- these modes propagate along the ice cover and interact again and again with the same heterogeneities and partially convert to slow flexural waves, and so on.

The amplitude of the primary flexural waves is extremely high; therefore the converted waves possess significant amplitudes and overlap the target reflections because they are multiply generated by random heterogeneities of the ice-water interface.

Acknowledgements

This work was supported by RSF (project No. 17-17-01128). The research was carried out using the equipment of the shared research facilities of HPC computing resources at Lomonosov Moscow State University, Joint Supercomputer Center of RAS and the Siberian Supercomputer Center.

References

1. Bailey, A.: Shooting seismic from floating ice. *Petroleum News* **12**(5), 7–8 (2007)
2. J. Blanch, A. Robertson, and W. Symes.: Modeling of a constant q : Methodology and algorithm for an efficient and optimally inexpensive viscoelastic technique. *Geophysics* **60**, 176–184 (1995)
3. Carey, K.L.: Observed configuration and computed roughness of the underside of river ice, St. Croix River, Wisconsin. U.S.Geological Survey Research, Prof. Paper 550-B, Washington, 192–198 (1966)
4. P. Joly, J. Rodriguez: An Error Analysis of Conservative Space-Time Mesh Refinement Methods for the One-Dimensional Wave Equation. *SIAM J. Numer. Anal.***43**(2), 825859 (2006)
5. Henley, D.C.: Attenuating the ice flexural wave on arctic seismic data. *Crewes Research Report* **13**, 29–45 (2004)
6. Kostin, V., Lisitsa, V., Reshetova, G., Tcheverda, V.: Local time-space mesh refinement for simulation of elastic wave propagation in multi-scale media. *Journal of Computational Physics* **281**, 669–689 (2015)
7. P. Moczo, J. Kristek, and V. Vavrycuk, and R. J. Archuleta, and L. Halada. 3d heterogeneous staggered-grid finite-difference modeling of seismic motion with volume harmonic and arithmetic averaging of elastic moduli and densities. *Bulletin of the Seismological Society of America* **92**, 3042–3066 (2002)
8. Press, F., Ewing, M., Crary, A.P., Katz, S., Oliver, J.: Air-coupled flexural waves in floating ice. Part I and II. *Geophysical Research Papers* **6**, 3–45 (1950)
9. Vishevsky, D., Lisitsa, V., Reshetova, G. and Tcheverda, V.: Numerical study of the interface error of finite-difference simulation of seismic waves. *Geophysics* **79**(4), T213–T232 (2014)
10. J. Virieux, H. Calandra, and R.-E. Plessix. A review of the spectral, pseudo-spectral, finite-difference and finite-element modelling techniques for geophysical imaging. *Geophysical Prospecting* **59**, 794–813 (2011)